Transport Anomalies and Adaptative Pressure-Dependent Topological Constraints in Tetrahedral Liquids: Evidence for a Reversibility Window Analogue

M. Bauchy and M. Micoulaut

Laboratoire de Physique Théorique de la Matière Condensée, Université Pierre et Marie Curie, 4 Place Jussieu, F-75252 Paris Cedex 05, France

(Received 11 May 2012; published 25 February 2013)

Topological rigid constraints can be computed rather simply with changing composition and temperature but their estimation remains challenging for other thermodynamic variables. Here, the investigation of densified silicate liquids from molecular dynamics simulations combined with an analysis of radial and angular atomic excursions allows defining a pressure dependence of such constraints. Results show, that for a given composition, the dependence is nonmonotonic as it depends on the interplay between constraints broken by thermal activation and additional constraints arising from the increase of network connectivity under pressure. An anomalous behavior for oxygen bending constraints is obtained in the (P, T) map which connects to reported anomalies in transport properties and is identified as the pressure analogue of the stress-free Boolchand intermediate phase in rigidity driven by composition.

DOI: 10.1103/PhysRevLett.110.095501 PACS numbers: 61.43.Fs

From a mechanical viewpoint, the progressive stiffening of an amorphous network can be described rather accurately from the topology and the relevant interactions which constrain bonds and angles at the molecular level [1]. In the literature, this has led to a well-characterized rigidity percolation which has been observed in chalcogenide and oxide glasses with changing composition [1]. Such systems will indeed undergo a transition between a underconstrained flexible phase giving rise to local deformation modes and an overconstrained stressed rigid phase which is locked by its high bond connectivity. In this respect, Maxwell topological constraint counting, based on the enumeration n_c of bond-stretching (BS) and bond-bending (BB) interactions acting as constraints, has been the central ingredient for the theoretical framework [2]. The archetypal system which has served as the benchmark is the Ge_xSe_{1-x} binary system [3] showing experimentally a flexible phase for $x < 0.20$ and a stressed rigid phase for $x > 0.26$ while defining in between a stress-free Boolchand intermediate phase (reversibility window) with remarkable properties [4,5].

More recently, the introduction of temperature-dependent constraints has permitted to extend the zero temperature theory to $T \neq 0$, allowing for a description of network-forming liquids and a quantitative prediction of some physical and chemical properties [6] with changing composition x and temperature, the main input being the number of constraints per atom $n_c(x, T)$, depending now explicitly on temperature *via* a heuristic step function.

At this point, a natural question emerges. Can such topological constraints be defined as a function of another obvious thermodynamic variable, for example, pressure? The question is far than trivial, in contrast with the derivation of constraints from composition or temperature. In the former case, $n_c(x)$ is built straightforwardly [2,4] from the coordination numbers and the composition x of the network species. For the latter and for a given constraint i, the temperature behavior $q_i(T)$ has the following obvious properties $q_i(0) = 1$ and $q_i(\infty) = 0$ and $q_i(T) \equiv n_{c(i)}(x, T)/n_{c(i)}(x, T = 0)$. This definition simply highlights the fact that all constraints must be intact for the fully connected network at $T = 0$ and broken in a high temperature liquid. There have been some attempts to derive $q_i(T)$, mostly from energy landscape approaches [7,8].

In addition, the issue of establishing a topological constraint count for densified liquids appears to be of great importance as these systems display under certain conditions anomalous behaviors in structural, dynamical, or thermodynamic properties [9,10] which bear striking similarities with those observed in the intermediate phase at ambient pressure [11–13]. Such similarities underscore a possible common physical origin for the observed anomalies. But before a unified picture can be proposed, there is need of a precise computation of the number of rigid constraints n_c with pressure. Rigidity induced by pressure has been obtained in simple network formers from molecular simulations [14], although an explicit estimate of n_c at the same simple and elegant level as the one used for x was not reported. Establishing at least partially $n_c(x, T, P)$ or generalizing a function $q_i(T, P)$ is the purpose of the present Letter.

Here, it is shown from a combination of molecular dynamics simulations of silicates and an analysis of angular and radial excursions that topological constraints with pressure can be established in a neat way. For very high pressures, glasses and liquids are stressed rigid, whereas they are flexible at $P = 0$. Results show that under pressure change, moderate densified liquids adapt and reduce their number of BB constraints, thus, opening a pressure window between approximately 1 and 13 GPa at 2000 K.

The latter is the pressure analogue of the stress-free reversibility window obtained in compositional studies [4]. In the present pressure window, transport properties such as diffusion, viscosity, and related activation energies display an anomalous behavior, i.e., an extremum with pressure change. It, therefore, suggests that observed anomalies [10] may well be salient features of the intermediate Boolchand intermediate phase in the liquid state.

We have simulated in a (N, P, T) Ensemble a 3000 atomic system of a $2SiO_2Na_2O$ liquid and glass under various (P, T) conditions. The choice of the system is motivated by the fact that NS2 is flexible ($n_c < 3$) at low temperature [15] and will become stressed rigid under pressure due to the tetrahedral to octahedral conversion of the silicon environment [9,16] which increases the global network connectivity. The atoms interact *via* a two-body Teter potential which reproduces very accurately not only the structure [17] but also the dynamics [18]. The equations of motion have been integrated using a leap-frog Verlet algorithm with a time step of 2 fs. Starting from an initial temperature of 5000 K, a certain number of points (T, P) in the thermodynamic diagram have been selected and accumulated over a time interval of 2 ns, prior to the constraint analysis. The diffusion coefficient D_i (i = Si, O) has been computed from the long time limit of the mean-square displacement $D = \lim_{t\to\infty}\langle r^2(t)\rangle/6t$, whereas the viscosity has been calculated using the Green-Kubo formalism [19]. Details on the computation of the transport properties can be found in Ref. [18]. The investigation of the effect of pressure on structure, dynamics and vibrational properties is reported in Ref. [16].

In the following, we focus on the BB constraint of a bridging oxygen (BO)-centred angle which is defined by two adjacent $SiO_{4/2}$ tetrahedra. Over the simulated trajectory (2 ns), for a given BO atom k, the angular motion will lead to a single bond angle distribution $P_k(\theta)$ which can be characterized by a mean $\bar{\theta}_k$ and a second moment (or standard deviation σ_{θ_k}). When σ_{θ_k} is large (usually $\sigma_{\theta_k} > 15$–$20°$ [20]), it suggests that the bond-bending restoring force which maintains the angle fixed around $\bar{\theta}_k$ is ineffective. As a consequence, the associated BB topological constraint can be considered as broken. On the contrary, for low values of σ_{θ_k}, the corresponding angle acts as a constraint and will contribute to n_c.

When averaged over the whole system (i.e., the whole population of BO atoms), one will not only obtain the usual bond angle distribution centred at 144°, similarly to a standard computation [17], but also a distribution of standard deviations σ.

Figure 1 shows the distribution of BO-centred angular standard deviations in the 2000 K liquid for increasing pressures ($0 < P < 20$ GPa). At ambient pressure, a bimodal distribution is found, similarly to Ref. [20]. The low and high σ contribution (σ_i and σ_b) can be unambiguously assigned to intact and broken constraints, respectively.

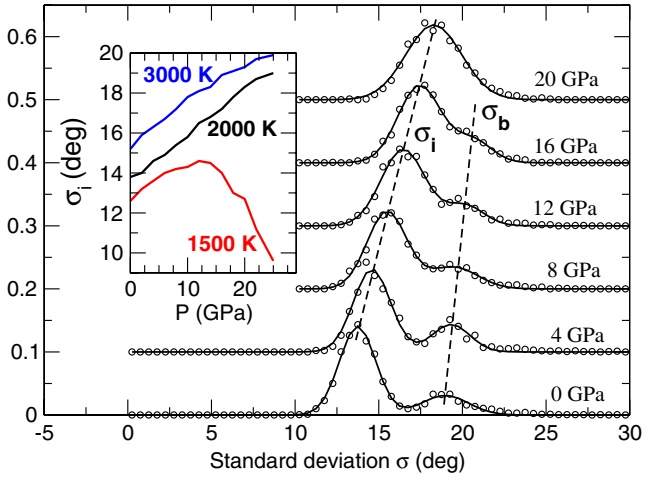

FIG. 1 (color online). Bridging oxygen (BO) standard deviation distribution in a simulated NS2 liquid at 2000 K for various pressures. Broken lines serve to track the peak positions σ_i and σ_b of the bimodal distribution. The behavior of the peak position σ_i with pressure is represented in the inset for different isotherms.

In fact, at low temperature (300 K, i.e., all constraints being intact) the standard deviation displays usually a sharp distribution centred at $\sigma_i < 10°$ [20], whereas at high temperature, where all rigid constraints are broken because of thermal activation [6], a broad distribution ($\sigma_b \simeq 25°$) is found. In the intermediate T interval, both contributions vary so that a bimodal distribution is obtained, as shown for $P = 0$ (Fig. 1). From the latter, one can estimate the fraction of intact BB constraints which is here equal to $q(2000\ \mathrm{K}) = 0.77$. With increasing pressure, two phenomena take place as shown from the evolution of the bimodal distribution (Fig. 1). First, the intensity of the peak centered at $\sigma = \sigma_b$ reduces before vanishing in the pressure range $16 < P < 20$ GPa. It is the signature that the thermally activated broken constraints are restored with applied pressure. The low σ contribution associated with intact constraints has a nearly constant intensity but shows a continuous shift of the peak position σ_i with P (inset of Fig. 1), indicative of an increased thermal activation but also of the presence of stress. In fact, it has been shown that angular standard deviations in Ge_xSe_{1-x} were increasing substantially when the network was undergoing the flexible to stressed rigid transition [21]. However, stress from applied pressure exceeds by far what can be achieved from a simple increase of connectivity [4]. In the low temperature liquid, stress cannot be released so that σ_i will first increase like in systems under compositional changes or in the present high temperature liquid containing a large fraction $q(T)$ of broken constraints. However, at low T, one has $q(T) \simeq 1$ so that additional pressure leads to a decrease of σ_i which results from the stiffening of the angular motion under high pressure. This trend can be correlated with the findings discussed below.

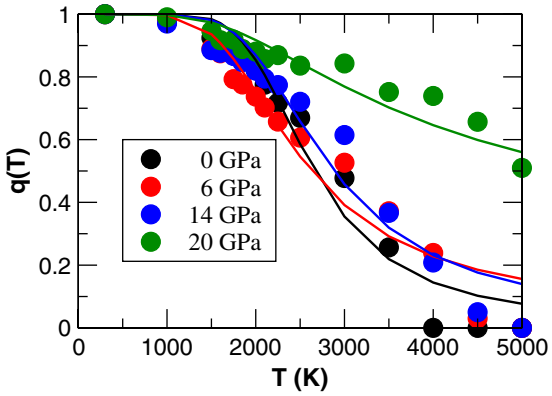

FIG. 2 (color online). Fraction $q(T)$ of intact angular (BB) constraints for different isobars in simulated NS2 liquids (symbols). The lines represent least-squares fit using Boltzmann prefactors (see text, for details).

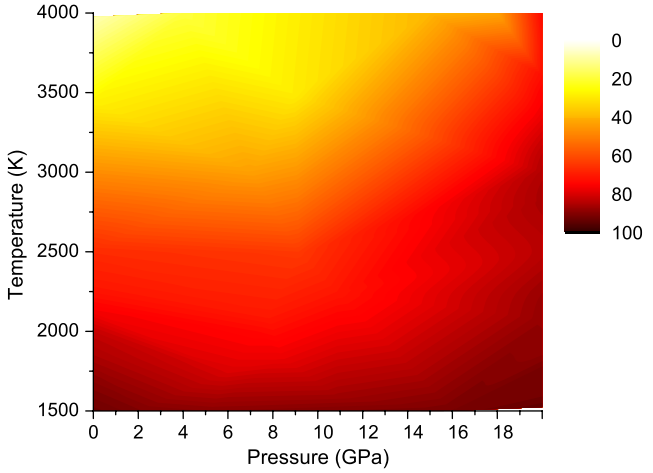

FIG. 3 (color online). Contour plot of the fraction (in %) of intact constraints $q(T, P)$ of liquid NS2 in the (T, P) map.

One can now track the fraction of intact constraints $q(T, P)$ along an isotherm or along an isobar. Figure 2 shows such computed fractions $q(T)$ at different fixed pressures, established from the respective populations contributing to the bimodal distribution (Fig. 1). At moderate pressures, all display a broad step like behavior, with $q(T)$ decreasing from one to zero when the temperature is increased. For very high pressures, $q(T)$ is found to decay only weakly with temperature and does not fall to zero even at the most elevated temperatures (5000 K). A least-squares fit (solid line in Fig. 2) to the numerical data at equilibrium ($T \leq 1500$ K) using a simple two-state model [22] involving Boltzmann prefactors $\exp[-U/k_BT]$ satisfying $q(0) = 1$ and $q(\infty) = 0$ shows that for $P = 0$, 6, and 14 GPa, the activation energy U necessary to break a constraint is equal to 0.61 ± 0.08, 0.40 ± 0.05, and 0.53 ± 0.07 eV, respectively. Thus, U passes through a minimum suggesting that thermally activated constraints can break more easily in a certain pressure interval.

Such a behavior can be quantitatively represented on a (P, T) map (Fig. 3) or with pressure along an isotherm [black curves, Fig. 4(a)]. In Fig. 3, a clear minimum is found at low temperatures in a pressure window approximately located over the interval $1 < P < 13$ GPa for 2000 K. Note that the width of the window decreases with decreasing temperature and is found to be centered at around 5 GPa at 1500 K, i.e., at the same pressure where a thermodynamic anomaly has been found in silica (negative dilatation coefficient [9]). The present anomaly appears to be the result of an interplay between the increase of connectivity arising from the tetrahedral to octahedral coordination change under pressure [18] which leads to additional stress and the softening of the bond-bending BO constraints which reduces rigidity. At ambient pressure, the NS2 glass and corresponding liquids are flexible ($n_c = 2.56$ at low temperature [15]). With the increase of pressure, the average silicon and oxygen coordination numbers $\bar{r}_{Si}$ and $\bar{r}_O$ increase (growth of Si^V, Si^{VI}, and O^{III} species [16]), leading to an increase of the number of constraints per atom by $\Delta n_c = 0.50$ when P increases from 0 to 10 GPa (and $\bar{r}_{Si}$ from 4.0 to 4.2). At the level of the network, the global increase of n_c arising from the growth of $\bar{r}_{Si}$ can be reduced during a certain pressure interval by breaking the energetically softer BB constraints of the BO atoms so that $q(P)$ decreases at low pressure [Fig. 3 and 4(a)]. However, with growing pressure (and still growing $\bar{r}_{Si}$ and $\bar{r}_O$), this adaptive behavior can only hold up to a certain point ($\simeq 13$ GPa at 2000 K), beyond which the softening of the BB constraints can not accomodate any more the steadily increasing pressure-induced stress. As a consequence, the BO bending motion will stiffen under pressure, resulting in an increase of $q(P)$ for $P > 13$ GPa. In this respect, the observed features bear large similarities with the self-organized Boolchand intermediate phase where growing stress induced by composition is released in adaptive networks maintaining $n_c \simeq 3$ over a finite compositional interval up to the stress transition [4].

Furthermore, the behavior of $q(P)$ is found [Fig. 4(a)] to be deeply correlated with a certain number of reported transport anomalies in tetrahedral liquids [9,10,18]. Figure 4 summarizes what has been found from molecular simulations at the temperature of 2000 K for the present NS2 liquid. In the pressure window where BB constraints break partially and reduce from $q(P) = 0.82$ to 0.72 at 6 GPa [Fig. 4(a)], in order to adapt for the increasing pressure-induced stress, viscosity and diffusion are found to be minimum and maximum, respectively. The Arrhenius plot of the viscosity or the diffusion constant (i.e., representing $D_{Si,O}$ or η with inverse temperature) permits us to follow the corresponding activation energies for viscous flow (E_A^η) or oxygen diffusion (E_A^D) as a function of pressure and these are also found to be minimum in the same pressure window as $q(P)$ for $T = 2000$ K and 1500 K, reducing from 1.6–1.4 eV to 1.1 eV, directly correlated

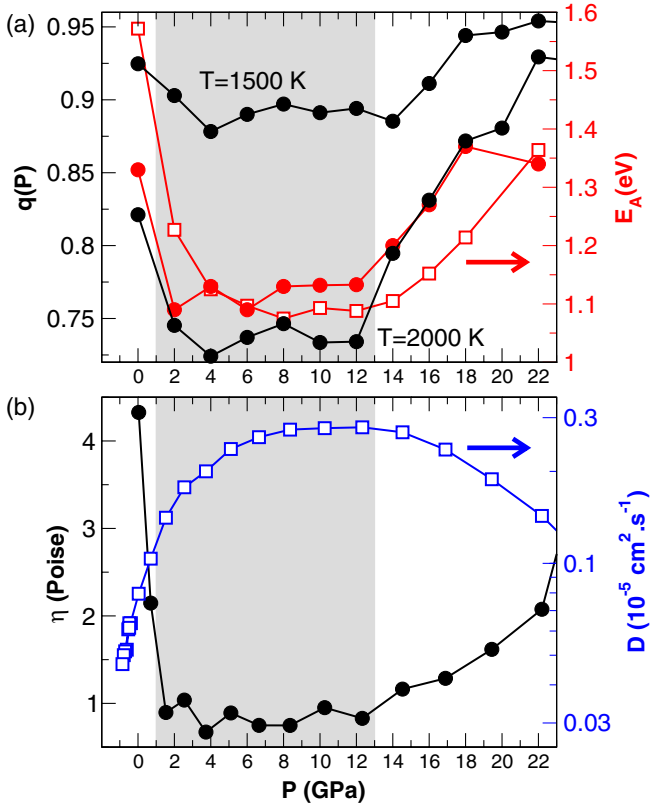

FIG. 4 (color online). (a) Behavior of the step function $q(P)$ in liquid NS2 for two isotherms ($T = 1500$ K and 2000 K, black curves) compared to the computed activation energy (right axis) for viscous flow E_A^η, (filled red circles) and for oxygen diffusion E_A^D (open red squares). (b) Computed viscosity $\eta(P)$ as a function of pressure for $T = 2000$ K. See also Ref. [18]. Right axis: Oxygen diffusion constant (blue symbols) $D_O(P)$. The grey area represents an approximate delimitation of the intermediate phase based on the window defined by the trend in $q(P,$ 2000 K).

with the trend obtained for $q(P)$. It underscores the fact that BB constraint adaptation is intimately related to the lowering of the energy barriers involved in viscous flow.

The pressure window appears to be the interval where, obviously, certain anomalies in the liquid take place and the constraint behavior suggests that it is the pressure analogue of the Boolchand phase or reversibility window where viscosity and E_A^η anomalies [5,23] have been observed as well. Therefore, several more general comments can be drawn in conclusion which connect to relaxation, the glass transition phenomenon, and the notion of optimal glasses.

First, it has been observed [24] that the glass-forming tendency is increased for systems that are able to increase their melt viscosity down to lower temperatures. For this reason, glasses form more easily at eutectics because freezing-point depressions bring the system to lower temperatures and higher viscosities, and this correlates rather well with observed minima in the critical cooling rate in order to avoid crystallization in NS liquids [25]. Following this observation, one should expect that along an isotherm, glass-formation will be optimized for systems having a lower viscosity [Fig. 4(b)]. This property will indeed allow the system found in the range $1 < P < 13$ GPa to reach lower temperatures at $\eta = 10^{12}$ Poise, i.e., viscosity of the glassy state. We have not computed the evolution of the numerical glass transition temperature T_g with pressure and can, therefore, not rescale the behavior of $\eta(1/T)$ to $\eta(T_g/T)$ at fixed pressure to estimate the liquid fragility $\mathcal{M}(P)$. However, given the known formula [12]: $\mathcal{M}(P) = E_A^\eta(P)\ln_{10}2/k_B T_g(P)$ and assuming that T_g does not depend too much on pressure, one may expect that in the present system the pressure window coincides with a minimum in fragility. This conclusion parallels the one derived from a simplified Kirkwood-Keating model of the glass transition [12] showing that glass-forming liquids in the Boolchand intermediate phase are strong and that activation energy for viscosity or relaxation time are minimum when $n_c \simeq 3$.

Second, one should mention the role played by composition such as in the archetypal Ge_xSe_{1-x} system. Here, for a given composition of a silicate system, we have shown that a subtle interplay can take place between pressure-induced stress and the softening of topological constraints by thermal activation. It becomes now clear that, ultimately, a rigidity map can be established for any ionocovalent compound from the estimate of the number of constraints $n_c(x, T, P)$, defining flexible, intermediate and stressed rigid zones in the thermodynamic diagram. At present, only some areas of this map have been characterized for sodium silicates: at fixed composition (NS2, present work), at zero pressure and zero temperature [15], and at zero pressure and fixed composition [20].

[1] *Rigidity Theory and Applications*, edited by M. F. Thorpe and P. M. Duxbury (Plenum Publishers, New York, 1999).
[2] M. F. Thorpe, J. Non-Cryst. Solids **57**, 355 (1983).
[3] X. W. Feng, W. J. Bresser, and P. Boolchand, Phys. Rev. Lett. **78**, 4422 (1997).
[4] M. Micoulaut, J. C. Phillips, Phys. Rev. B **67**, 104204 (2003).
[5] S. Stolen, T. Grande, and H. B. Johnsen, Phys. Chem. Chem. Phys. **4**, 3396 (2002).
[6] P. K. Gupta and J. C. Mauro, J. Chem. Phys. **130**, 094503 (2009).
[7] G. Foffi, J. Phys. Condens. Matter **20**, 494241 (2008).
[8] A. Huerta and G. G. Naumis, Phys. Rev. B **66**, 184204 (2002).
[9] K. Trachenko, M. T. Dove, V. V. Brazhkin, and F. S. El'kin, Phys. Rev. Lett. **93**, 135502 (2004).
[10] M. S. Shell, P. G. Debenedetti, and A. Z. Panagiotopoulos, Phys. Rev. E **66**, 011202 (2002); B. Shadrack Jabes, M. Agarwal, and C. Chaktavarty, J. Chem. Phys. **132**, 234507 (2010).

[11] C. Bourgel, M. Micoulaut, M. Malki, and P. Simon, Phys. Rev. B **79**, 024201 (2009).
[12] M. Micoulaut, J. Phys. Condens. Matter **22**, 285101 (2010).
[13] A. N. Sreeram, A. K. Varshneya, and D. R. Swiler, J. Non-Cryst. Solids **128**, 294 (1991).
[14] K. Trachenko and M. T. Dove, Phys. Rev. B **67**, 212203 (2003).
[15] M. Micoulaut, Am. Mineral. **93**, 1732 (2008).
[16] M. Bauchy, J. Chem. Phys. **137**, 044510 (2012).
[17] A. N. Cormack, J. Du, and T. R. Zeitler, Phys. Chem. Chem. Phys. **4**, 3193 (2002).
[18] M. Bauchy and M. Micoulaut, Phys. Rev. B **83**, 184118 (2011); M. Bauchy, B. Guillot, M. Micoulaut, and N. Sator, Chem. Geol. (in press).
[19] M. P. Allen and D. J. Tildesley, *Computer Simulations of Liquids* (Oxford University, Oxford, 1987).
[20] M. Bauchy and M. Micoulaut, J. Non-Cryst. Solids **357**, 2530 (2011).
[21] A. Alam, R. K. Chouhan, and A. Mookerjee, Phys. Rev. B **83**, 054201 (2011).
[22] C. A. Angell, B. E. Richards, and V. Velikov, J. Phys. Condens. Matter **11**, A75 (1999).
[23] D. G. Georgiev, P. Boolchand, and M. Micoulaut, Phys. Rev. B **62**, R9228 (2000).
[24] P. Richet, M. Roskosz, and J. Roux, Chem. Geol. **225**, 388 (2006).
[25] C. Y. Fang, H. Yinnon, and D. R Uhlmann, J. Non-Cryst. Solids **57**, 465 (1983).